In Situ, Real-Time FT-IR/CIR/ATR Study of the Biocorrosion of Copper by Gum Arabic, Alginic Acid, Bacterial Culture Supernatant and *Pseudomonas atlantica* Exopolymer

JOHN G. JOLLEY,* GILL G. GEESEY, MICHAEL R. HANKINS, RANDY B. WRIGHT, and PAUL L. WICHLACZ

Idaho National Engineering Laboratory/EG&G Idaho, Inc., Idaho Falls, Idaho 83415 (J.G.J., M.R.H., R.B.W., P.L.W.); and Department of Microbiology, California State University, Long Beach, CA 90840 (G.G.G.)

Thin films (2.0 nm) of copper on germanium internal reflection elements (IREs) were exposed to 10% gum arabic (aqueous solution), 2% alginic acid (aqueous solution), 1% bacterial culture supernatant (BCS, simulated seawater solution), and 0.5% *Pseudomonas atlantica* exopolymer (simulated seawater solution) and monitored *in situ*, real time, with the use of Fourier transform infrared/cylindrical internal reflection/attenuated total reflection spectroscopy as a function of time at ambient conditions. Ancillary graphite furnace atomic absorption spectroscopy was used to monitor the removal process of the copper thin film from the germanium IREs. Results indicate that some of the copper was removed from the Cu/Ge interface by all four polymers and incorporated into the polymer matrix. Thus, biocorrosion of copper was exhibited by the four polymers in the order of alginic acid > gum arabic > BCS > *Pseudomonas atlantica* exopolymer. The FT-IR/CIR/ATR technique can be successfully used to monitor biocorrosion systems in *in situ*, real-time settings.

Index Headings: **Cylindrical internal reflection; Fourier transform infrared spectroscopy; Biocorrosion; Gum arabic; Alginic acid; Bacterial culture supernatant; *Pseudomonas atlantica*; Exopolymer; Metal thin-film deposition techniques.**

INTRODUCTION

When a surface becomes exposed to a nonsterile environment, a series of chemical and biological events can occur, resulting in surface microbial colonization and the propagation of microbial activities. The activity of microorganisms on surfaces can be beneficial (such as biomining) or deleterious (such as biofouling and biocorrosion). Biologically induced corrosion has been shown to be responsible for a significant portion of materials failure.[1-4]

In an attempt to gain a better understanding of the biological reactions that occur on surfaces under biofilms and, perhaps, exploit microbial activity, investigators have directed their attention to the near-surface region (μm range of interaction) using Fourier transform infrared/attenuated total reflection spectroscopy (FT-IR/ATR).[5-15] This approach had led to the finding that bacterial exopolysaccharides which anchor the cells to surfaces (see Fig. 1) also promote the destruction of the surface.[16, 17] X-ray photoelectron spectroscopy (XPS) and Auger electron spectroscopy (AES) make it possible to examine such surface (nm range of interaction) phenomenon.[18,19]

In this work gum arabic (GA), alginic acid (AA), bacterial culture supernatant (BCS), and *Pseudomonas atlantica* (*Pa*) exopolymer interactions with copper were investigated with FT-IR/CIR/ATR to further elucidate the nature of the destruction of a copper surface exposed to exopolysaccharides from surface-colonizing *P. atlantica* and LST bacteria (*P. atlantica* and BCS exopolymers, respectively), and acidic polysaccharides from kelp and from the Acacia tree (alginic acid and gum arabic, respectively. *P. atlantica* was chosen because it is a common marine microbe that has been isolated from colonized metal surfaces. It is suspected to have an active role in biocorrosion/fouling processes. The BCS from the LST microbe has been shown to stimulate settlement of marine larvae. Concern has been raised over possible biocorrosion/fouling of metal surfaces if used in marine environments.

EXPERIMENTAL

Sample Preparation. The surface of the Ge IREs and discs were polished with a sequence of 400 grit SiC paper, 600 grit SiC paper, 6 μm diamond paste, 1 μm diamond paste, 0.3 μm alumina, and 0.05 μm alumina. Polishing cloth was used with a diamond paste and alumina. All polishing materials were manufactured by Buehler. In order that the IREs could be rotated during polishing, one of the IRE ends was covered with Teflon® tape and installed into a variable-speed drill. After completion of the polishing step, the other end was taped, installed, and polished as before. Optical microscopy was used to determine the polishing starting point and the progress of the polishing in each step. Thin films (2.0 nm on the IREs and rods, 3.4 nm on the discs and slides) of copper were deposited on Ge IREs from Spectra-Tech [6.35-mm diameter × 82.6-mm length with 30° (with respect to axis) end cones], Ge discs (6.35-mm diameter × 1-mm thick), Pyrex® microscope slides, and Pyrex® rods (6.35-mm diameter) in an Enerjet Model UCV-18/6 magnetron sputtering system. The Ge discs were made from broken Ge IREs. Substrates (IREs, discs, slides, and rods) were mounted on Teflon® fixtures in the vacuum chamber (see Fig. 2). The discs and microscope slides were held stationary while the IREs and rods were rotated by the rotary feed-through at 78 rpm. The ends of the IREs were capped with Teflon® caps to protect the IRE end cones from being coated during sputtering. Target ma-

Received 15 June 1988; revision received 3 February 1989.
* Author to whom correspondence should be sent.

0003-7028/89/4306-1062$2.00/0

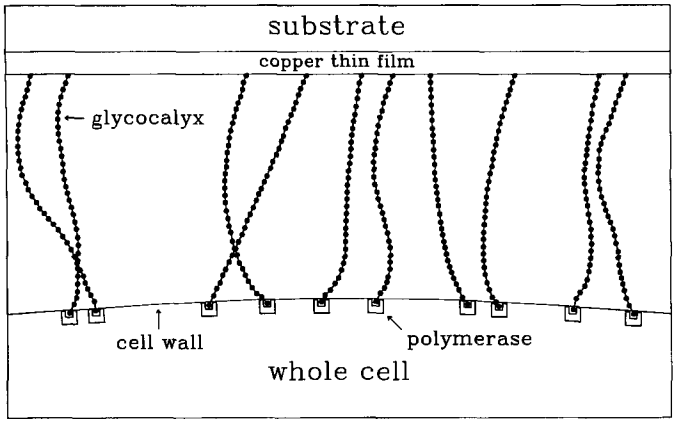

FIG. 1. Schematic of whole cell attached to surface. (Note: not to scale.) The glycocalyx is comprised of long chains of polysaccharides that are formed by bacterial enzymes called polymerases (C-shaped structures). The polymerases are affixed at or near the cell surface. The whole cell uses this structure network to adhere to a nearby surface (e.g., copper thin film).

terial consisted of 99.999% pure copper supplied by the Kurt J. Lesker Co. A pumpdown pressure of 2×10^{-7} Torr was achieved before sputtering. Neon working gas (99.99% pure from Matheson Gas Products) was introduced into the sputtering chamber at a pressure of 30 mTorr. The deposition rate was 0.12 nm s^{-1}. A quartz crystal oscillator, manufactured by the R. D. Mathis Co., was used to monitor the Cu thin-film thickness, while graphite furnace atomic absorption spectroscopy (GFAAS) was used for analysis of the Cu thickness on the slides and rods for system calibration. A shutter assembly was used to allow the target surface to be sputter-cleaned before deposition. After two minutes of sputtering, the shutter was opened to allow deposition of the copper onto the substrates. Substrates were at ambient temperature during sputtering. Auger maps with 200-nm lateral resolution (copper LMM at 920 eV and germanium LMM at 1147 eV) were used to evaluate the uniformity of the copper thin film on the substrate. The films appeared to be continuous, void of island effects or porosity. XPS analysis of the copper thin films indicated that the copper was in the zero valent reduced state and thus was not detectably oxidized prior to solution exposure.[18,20]

Saturated polysaccharide suspensions were prepared from dehydrated preparations. Gum arabic (Aldrich, 26,077-0) was prepared as a 10% w:v solution in 18 MΩ nanopure (np) water (obtained from a Barnstead NANOpure II water system); the pH was adjusted to 7.0 with dilute HCl and NaOH, sterilized by filtering through a 0.45-μm-pore-size membrane, and frozen at −70°C for storage. Alginic acid (Sigma, A-7003) was prepared as a 2% w:v solution, as above. Exopolymer from a bacterial culture of *P. atlantica* was obtained by sedimenting the cells by centrifugation and treating the supernatant liquid with two parts 2-propanol at 4°C overnight. The precipitated exopolysaccharide was redissolved in np water, dialyzed (to reduce cation concentration by diffusion through a semipermeable membrane)[21] against np water, and then lyophilized (freeze dried). A 0.5% suspension of the lyophilized material was prepared as described above for the gum arabic, except that AQUIL simulated

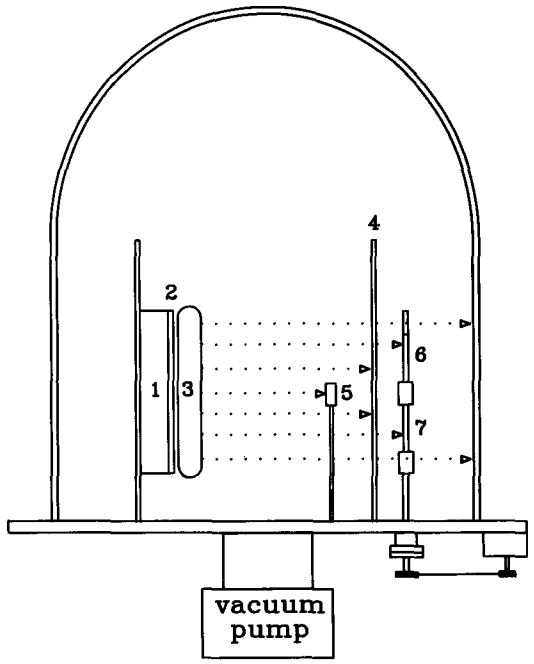

1: gun, 2: target, 3: plasma, 4: shutter, 5: quartz crystal oscillator, 6: Pyrex rod, 7: IRE

FIG. 2. Sputtering system configuration for substrate deposition. The magnetron sputtering system was configured for the deposition of Cu on IREs, Pyrex® rods, and Ge discs. A rotary feedthrough was coupled to a low-rpm electric motor for rotation of the IREs and Pyrex® rods.

seawater (ss water, pH of 7.6) was used in place of np water. The composition for AQUIL ss water is shown in Table I. The supernatant fraction (BCS) from a stationary-phase culture of a marine bacterial isolate referred to LST, grown in liquid medium composed of Brain Heart Infusion Broth and 3% NaCl, was obtained by centrifugation and then lyophilized. BCS was rehydrated in ss water as a 1% suspension and filtered and frozen as above.

Fourier Transform Infrared Spectroscopy. Cu deposited Ge IREs were placed into the stainless-steel open-boat CIRCLE cell (from Spectra-Tech). The cell was installed into the CIRCLE mirror assembly in the FT-IR optical bench (while under purge with LN_2 boil off). Seven mL (by 20 mL syringe) of each of the polymer solutions and ss water (np water was used as the control) were placed into the cell. The 7-mL volume completely covered the IRE. As soon as the CIRCLE cell cover was installed, infrared spectra were immediately collected by a Digilab FTS-15C FT-IR spectrometer at one-minute

TABLE I. AQUIL (simulated) seawater composition.

Reagent	gm/L added
$CaCl_2 \cdot 2H_2O$	1.54
$MgCl_2 \cdot 6H_2O$	11.1
NaCl	24.53
$SrCl_2 \cdot 6H_2O$	0.017
KBr	0.10
$NaHCO_3$	0.20
KCl	0.70
H_3BO_3	0.03
NaF	0.003
Na_2SO_4	4.09

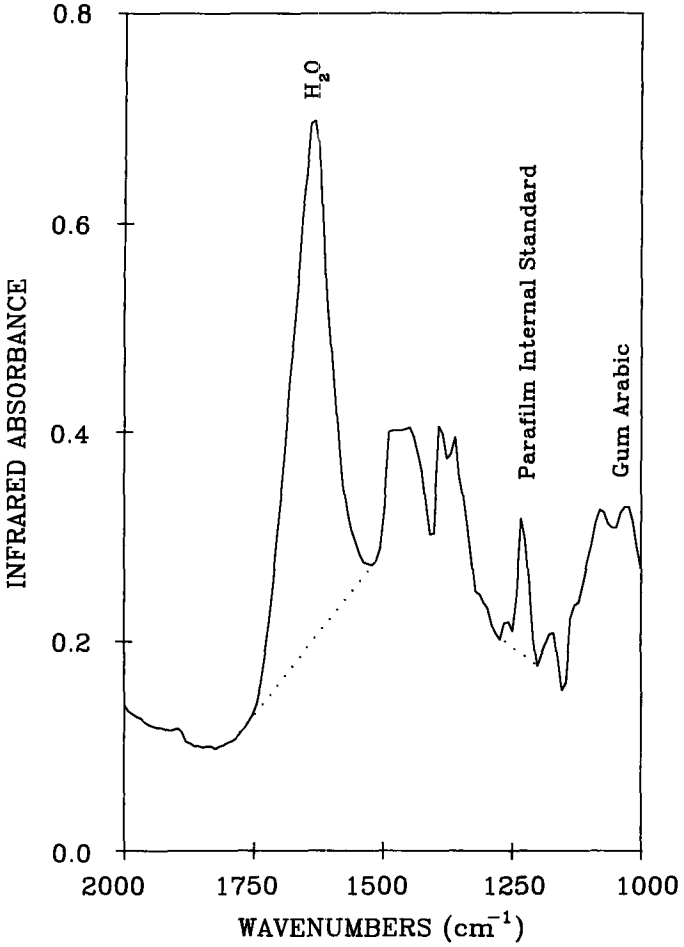

FIG. 3. FT-IR/CIR/ATR spectra of 10% gum arabic solution. The Parafilm strip was installed into the optical light path after the CIRCLE attachment. The dotted lines represent the integration baseline parameters used.

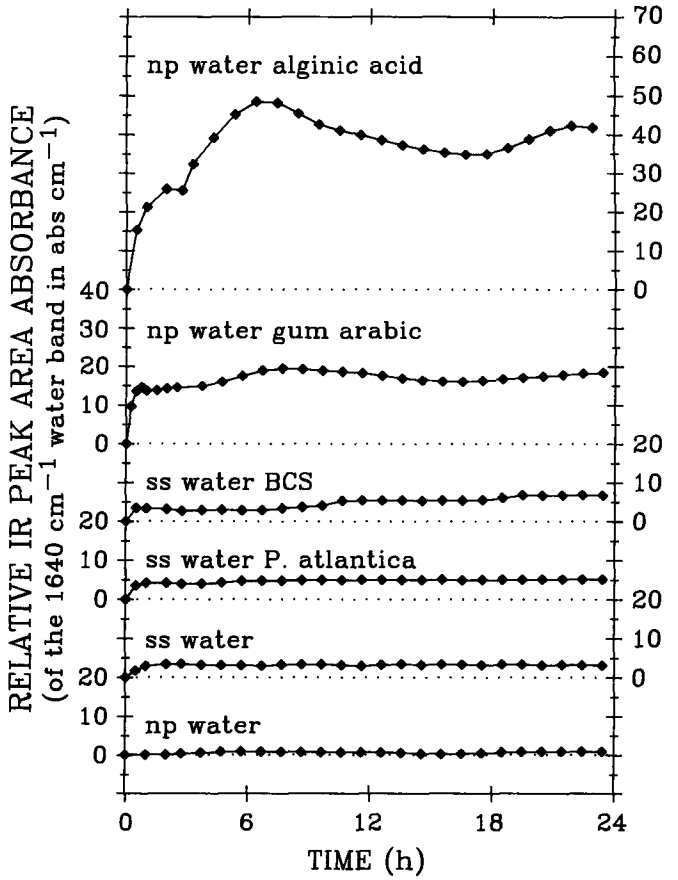

FIG. 4. Plot of IR peak area absorbances. Relative IR peak area absorbances of the 1640-cm^{-1} water band were determined as a function of Cu/polymer solution exposure time.

intervals for one hour, fifteen-minute intervals for two hours, and one-hour intervals for a total of 24 h. The FT-IR was equipped with a mercury-cadmium-telluride (MCT) narrow-range detector. Spectra were collected with a resolution of 8 cm^{-1}, with 50 co-added scans, and with a mirror velocity of 0.15 cm s^{-1}.

Because the intensity of the band increases as the thickness of the copper thin film decreases, the 1640-cm^{-1} water absorbance band was monitored as a function of time. Peak areas for the 1640-cm^{-1} water absorbance band were determined (see Fig. 3 for example of spectra). For normalization of the spectra as a function of time, a 6-mm-wide strip of Parafilm (manufactured by American Can Co.) was placed in the IR light path after the CIRCLE attachment, to serve as an internal standard. Parafilm was chosen since the spectral bands did not overlap with the experimental bands of interest. The resulting data were plotted as a function of time (see Fig. 4).

Graphite Furnace Atomic Absorption Spectroscopy. The Cu thin films that were deposited on the microscope slides and rods were dissolved with concentrated HNO_3. (Note: concentrated HNO_3 will chemically attack the Ge IRE, leading to pitting of the surface.) Np water was used for rinsing. The resulting solutions were quantitatively transferred to 10-mL volumetric flasks. Aliquots (0.020 mL) of solutions (diluted as required for the linear absorbance range) were pipetted (with an Eppendorf pipet) into the L'vov-platform-equipped Perkin-Elmer HGA-400 graphite furnace which was installed in a Perkin-Elmer 703 atomic absorption spectrometer. The resulting concentration determinations were then used to calculate the Cu thin-film thickness for the Ge substrates and quartz crystal oscillator response. The density of the Cu was assumed to be 8.93 gm cm^{-3}.

Cu-deposited Ge discs were placed into analytically clean (leached for 24 h in 10% HNO_3, rinsed with np water) vials. One mL (pipetted by Eppendorf pipet) of each of the polymer solutions and ss water (np water was used as the control) was placed into the corresponding vial for copper/solution exposure (24 h duration) at ambient temperature. At the end of the exposure time period, the Ge discs were removed from the vials with analytically clean plastic hemostats. The np water used to rinse the Ge discs was not added to the vials, in order to minimize any Cu erosion contribution from the rinsing process. Exposed polymer and water solutions were kept for subsequent GFAAS analysis.

Due to matrix effects (light scatter from polymer smoke) exhibited by the polymers, an electrochemical separation technique was used to isolate the copper from the bulk of the polymer solution.[22] The polymer solutions were transferred to an analytically clean beaker, diluted to 80 mL with np water, and acidified with 0.50 mL of

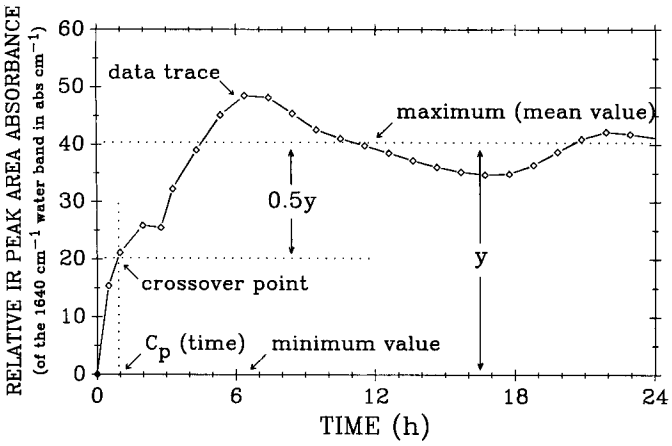

FIG. 5. C_p determination example for FT-IR/CIR/ATR profile. The alginic acid FT-IR/CIR/ATR data were used in this example.

concentrated H_2SO_4. Two analytically clean platinum electrodes were placed into the resulting solutions, and a 2.6-V potential was applied across the electrodes with a JQE 0–6 V, 0–10 A Kepco power supply. The Cu which was plated onto the Pt cathode electrode was dissolved off with 10% HNO_3. The resulting solutions were analyzed by GFAAS, as above. Copper-spiked controls (polymer solutions) were used to evaluate the separation yields. The control data indicated a 93% separation yield. The resulting concentration determinations were then used to calculate the yield of Cu, which was incorporated into the polymer solution from the Cu deposited upon the Ge substrates.

RESULTS AND DISCUSSION

Fourier Transform Infrared Spectroscopy. If one uses Harrick's equation (which is as follows:

$$d_p = \lambda/[2\pi n_1(\sin^2\theta - n_{21}^2)^{1/2}] \quad (1)$$

where λ is the wavelength of the radiation in air, θ is the angle of incidence, n_1 is the refractive index of the IRE, and n_{21} is the ratio of the refractive index of the sample divided by that of the IRE) to determine the approximate depth of penetration of the evanescent wave (defined as the distance required for the electric field amplitude to fall to e^{-1} of its value at the surface) and assumes that $\theta = 45°$, $\lambda = 6.1$ μm (wavelength corresponding to the 1640 cm^{-1} water absorbance band), $n_2 = 4.0$, and $n_{21} = 0.38$ ($n_2 = 1.5$ for water), the effective penetration depth of the electric field is 0.41 μm for the uncoated Ge IRE.[6,9,23] On the basis of 10 reflections in the IRE, the effective transmission cell pathlength is 12 μm.[8] The penetration depth is reduced (also the effective cell pathlength) by the addition of a metal thin film onto the surface of the IRE. This is due to the relatively high refractive index (2 to 20) and absorptivity of metals with regard to infrared radiation. The 1640-cm^{-1} water absorbance band was not detectable when the Ge IRE was coated with >4.1 nm of copper (these findings were in agreement with those of Iwaoka *et al.*).[6] As the copper thin film is removed from the IRE, the effective cell pathlength of the evanescent wave is increased, resulting in an increased 1640-cm^{-1} water absorbance band. Thus, the copper removal from the IRE by test solutions can be profiled by monitoring the change (Δ) in the 1640-cm^{-1} water absorbance band peak area as a function of time. The calculations assume that n_2 remains constant at the IRE near-surface (μm) region.

TABLE II. FT-IR/CIR/ATR corrosion data.

Sample	C_p time (min)	Δ Peak area (abs cm^{-1})	Rate of change (abs cm^{-1} min^{-1})	Percent Cu removed
Cu/AA	55.2	40.3	0.4	64
Cu/GA	14.9	17.7	0.6	38
Cu/BCS[a]	29.4	6.7	0.1	19
Cu/*Pa*[a]	21.2	0.5	0.01	14
Cu/H_2O[a]	27.8	0.3	0.005	11
Cu/H_2O	N.D.	<0.1	N.D.	<5

[a] Simulated seawater.

The water absorption profiles and data of the removal of Cu by water (np and ss), gum arabic, alginic acid, BCS (in ss water), and *P. atlantica* (in ss water) solutions are shown in Fig. 4 and summarized in Table II. To facilitate comparison of the profiles, we determined C_p (cross-over point) values to describe the amount of time required for the reaction to proceed 50% of the maximum change. The C_p results were calculated by determining the time where the half-distance (0.5y, where y equals the total distance between the maximum and minimum Δ peak areas) crosses the trace of the data (see Fig. 5). The rate of change was determined by dividing the Δ peak area with $2C_p$. The np water and ss water C_p values were (1) not detectable and (2) 27.8 min, respectively; the Δ peak areas were < 0.1 and 0.3 abs cm^{-1}, respectively. The rates of change were (1) not detectable and (2) 0.005 abs cm^{-1} min^{-1}. These data indicate that the Cu thin film was relatively stable while being exposed to np water but was attacked to a limited extent by the ss water during the 24 h exposure time.

The *P. atlantica*, BCS (both in ss water), gum arabic, and alginic acid C_p values were 21.2, 29.4, 14.9, and 55.2 min, respectively. The Δ peak areas were 0.5, 6.7, 17.7, and 40.3 abs cm^{-1}, respectively. The rates of change were 0.01, 0.1, 0.6, and 0.4 abs cm^{-1} min^{-1}, respectively. The data indicate that the four polymer solutions were able to remove some of the deposited Cu. Geesey *et al.*[24] reported water absorption profiles from experiments in which they used physical vapor deposition (PVD) to de-

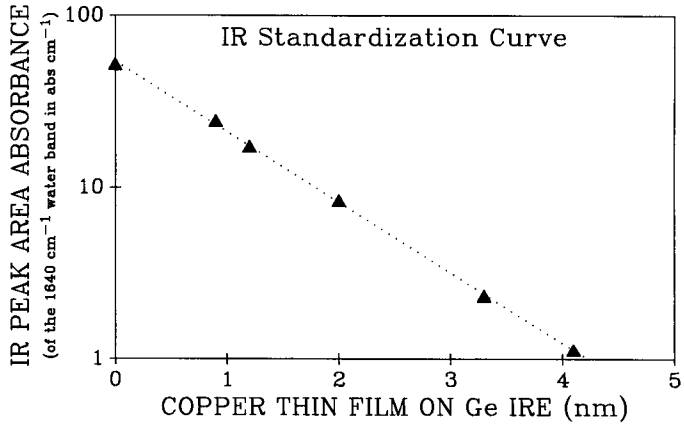

FIG. 6. Calibration curve for FT-IR/CIR/ATR response as a function of copper thin-film thickness.

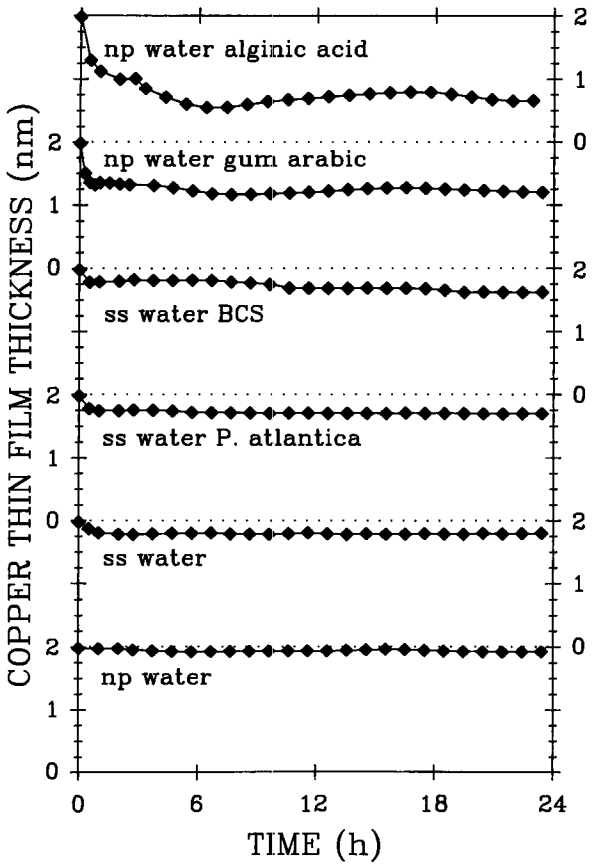

FIG. 7. Calculated copper thin-film thickness profiles as a function of time.

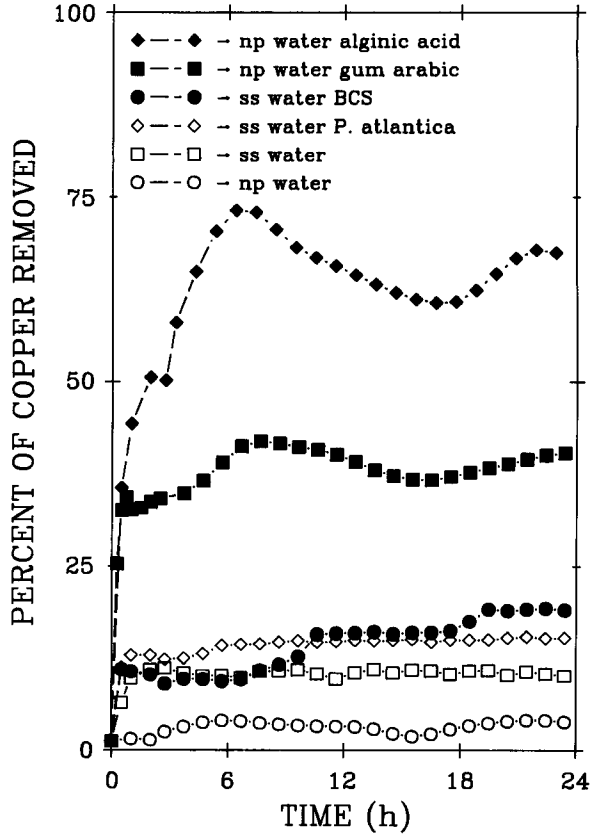

FIG. 8. Percent of copper removed as a function of time.

posit the thin film of copper upon the Ge IREs. Comparison of the profiles indicates a close similarity of the results and trends, even though different equipment and thin-film deposition techniques were used.

To transform the water absorption profiles to copper thin-film thickness profiles, we deposited a set of standard thicknesses (0.9, 1.2, 2.0, 3.3 and 4.1 nm) of copper thin films upon the Ge IREs and exposed them to np water. The resulting IR peak area absorbance values for the 1640-cm^{-1} water band are shown in Fig. 6 as a function of the Cu thin-film thickness. A first-order regression was applied to the semi-log data, to form the calibration curve. The thickness of the copper thin films used during the test solution exposures was calculated by using the integrated water absorption band profile data in the calibration curve expression. The resulting copper thin-film thickness profiles and data for the removal of Cu by water and the four polymer solutions are shown in Fig. 7 and summarized in Table II. Of the total Cu available, 64, 38, 19, 14, 11 and <5% were removed from the substrate by the alginic acid solution, gum arabic solution, BCS solution, *P. atlantica* exopolymer solution, ss water, and np water, respectively, and incorporated into solution. These data indicate that the four polymer solutions were able to remove some of the deposited Cu in the order of alginic acid > gum arabic > BCS > *P. atlantica* (see Fig. 8). The wavy character during equilibrium is believed to be due to the agglutination and subsequent slough process.

Graphite Furnace Atomic Absorption Spectroscopy. The quantitative evaluations by GFAAS of the removal of Cu for the water and four polymer solutions are summarized in Table III. Less than 0.1% of the total available Cu was removed from the substrate and solubilized into the water during 262 h of exposure to np water. This result indicates that the Cu thin film was relatively stable while being exposed to np water. The ss water was able to remove 3.5% of the copper from the substrate during the 24 h exposure time.

Of the total Cu available, 41, 36, 22, and 6.0% were removed from the substrate by the alginic acid solution, gum arabic solution, BCS solution, and *P. atlantica* exopolymer solution, respectively, and incorporated into the solution. One would expect to find that the above values are low (as compared to the true bulk concentration), since the disc rinse was not analyzed. The concentration of removed Cu would be expected to be higher at the near-surface disc/Cu thin-film region than in the bulk. Thus a significant Cu contribution may have been not accounted for. Nevertheless, the GFAAS data indicate the same general trends as the FT-IR/CIR/ATR deter-

TABLE III. Graphite furnace atomic absorption yield data.

Sample	Exposure time (h)	Percent Cu removed
Cu/AA	24	41
Cu/GA	24	36
Cu/BCS[a]	24	22
Cu/*Pa*[a]	24	6.0
Cu/H_2O[a]	24	3.5
Cu/H_2O	262	<0.1

[a] Simulated seawater.

minations—which was the purpose of the GFAAS analysis. The four polymer solutions were thus able to remove some of the deposited Cu in the order of alginic acid > gum arabic > BCS > *P. atlantica*—the same relative ordering as determined with the FT-IR/CIR/ATR technique.

SUMMARY

FT-IR data (supported by the GFAAS data) indicate that the copper thin film was relatively stable while being exposed to np water but was removed to a small extent by the ss water. Some of the copper was removed from the Cu/Ge interface by all four polymers and incorporated into the polymer matrix. Thus, biocorrosion of copper was exhibited by gum arabic, alginic acid, BCS, and *Pseudomonas atlantica* exopolymer. The FT-IR/CIR/ATR technique can be successfully used to monitor biocorrosion systems, in an *in situ*, real-time manner.

ACKNOWLEDGMENTS

We would like to acknowledge Debby F. Bruhn and Clyde R. Toole of the Idaho National Engineering Laboratory/EG&G Idaho, Inc. for technical discussion concerning this program and for ERDP (Exploratory Research and Development Program) management, respectively. We would also like to thank G. Abu, R. Weiner, and R. Colwell of the University of Maryland for the BCS preparation. This research was supported by the U.S. Department of Energy under DOE Contract No. DE-AC07-76ID01570 and NSF Grants ECE-8521693 and ECE-8701462.

1. B. Little and J. Jacobus, Org. Geochem. **8,** 27 (1985).
2. R. E. Baier, "Influence of the Initial Surface Condition of Materials on Bioadhesion," in *Proceedings of the Third International Congress of Marine Corrosion and Fouling* (National Institute of Standards and Technology, Gaithersburg, Maryland, 1972), p. 633.
3. M. J. Brown and J. N. Lester, Water Res. **13,** 817 (1979).
4. K. M. Hsieh, L. W. Lion, and M. L. Shuler, Appl. Environ. Microbiol. **50,** 1155 (1985).
5. V. A. DePalma and R. E. Baier, "Microfouling of Metallic and Coated Metallic Flow Surfaces in Model Heat Exchange Cells," in *Proceedings of the OTEC Biofouling and Corrosion Symposium* (Department of Energy, Washington, D.C., 1978).
6. T. Iwaoka, P. R. Griffiths, J. T. Kitasako, and G. G. Geesey, Appl. Spectrosc. **40,** 1062 (1986).
7. S. Winters, R. M. Gendreau, R. I. Leininger, and R. J. Jakobsen, Appl. Spectrosc. **36,** 404 (1982).
8. M. Sabo, J. Gross, J. Wang, and I. E. Rosenberg, Anal. Chem. **57,** 1822 (1985).
9. D. A. Saucy, S. J. Simko, and R. W. Linton, Anal. Chem. **57,** 871 (1985).
10. D. J. Fink and K. K. Chittur, Enzyme Microb. Technol. **9,** 568 (1986).
11. R. J. Jakobsen and D. G. Cornell, Appl. Spectrosc. **40,** 318 (1986).
12. J. S. Wong, A. J. Rein, D. Wilks, and P. Wilks, Jr., Appl. Spectrosc. **38,** 32 (1984).
13. R. M. Gendreau and R. J. Jakobsen, Appl. Spectrosc. **32,** 326 (1978).
14. R. M. Gendreau, K. K. Chittur, R. A. Dluhy, and T. B. Hutson, Am. Biotechnol. Lab. **5,** 10 (1987).
15. G. G. Geesey, M. W. Mittleman, T. Iwaoak, and P. R. Griffiths, Mater. Performance **25,** 37 (1986).
16. T. Rudd, R. M. Sterritt, and J. N. Lester, Water Res. **18,** 379 (1984).
17. G. G. Geesey, Am. Soc. Microbiol. **48,** 9 (1982).
18. J. G. Jolley, G. G. Geesey, M. R. Hankins, R. B. Wright, and P. L. Wichlacz, Surf. Interface. Anal. **11,** 371 (1988).
19. M. Rodriguez-Leiva and H. Tributsch, Arch. Microbiol. **149,** 401 (1988).
20. M. R. Pinnel, H. G. Tompkins, and D. E. Heath, Appl. Surf. Sci. **2,** 558 (1979).
21. M. W. Mittelman and G. G. Geesey, Appl. Environ. Microbiol. **49,** 846 (1985).
22. H. H. Willard, L. L. Merritt, Jr., J. A. Dean, and F. A. Settle, Jr., *Instrumental Methods of Analysis* (Wadsworth, Belmont, 1981). 6th ed., Chap. 5, pp. 146–149.
23. N. J. Harrick, *Internal Reflection Spectroscopy* (Wiley-Interscience, New York, 1967).
24. G. G. Geesey, L. Jang, J. G. Jolley, M. R. Hankins, T. Iwaoka, and P. R. Griffiths, Water Sci. Technol. **20,** 161 (1988).

Quantitative Analysis of Liquid Fuel Mixtures with the Use of Fourier Transform Near-IR Raman Spectroscopy

M. B. SEASHOLTZ, D. D. ARCHIBALD, A. LORBER,* and B. R. KOWALSKI†

Department of Chemistry, BG-10, University of Washington Seattle, Washington 98195

Near-infrared Fourier transform (near-IR FT) Raman spectroscopy was used to predict mass percentages of liquid fuel mixtures without the use of an internal standard. The 29 mixtures making up the calibration set were composed of varying mass percentages of unleaded gasoline, superunleaded gasoline, and diesel. Predictions were made with the use of classical least-squares with the pure components. Root mean square error (RMSE) values for all samples were 13.5, 13.8, and 5.2% (absolute error) for unleaded, superunleaded, and diesel, respectively. Using an estimate of the pure spectra determined by calibration gave RMSE values of 13.3% for unleaded, 12.2% for superunleaded, and 5.0% for diesel. A partial least-squares (PLS) model was able to partially compensate for matrix effects. Using different portions of the Raman spectra reduced the RMSE to 5.7% for unleaded, 5.2% for superunleaded, and 1.3% for diesel.

Index Headings: **Spectroscopy (near-IR, Raman, FT-IR, quantitative); Liquid hydrocarbon analysis; Partial least-squares; Multiple linear regression; Multivariate calibration.**

INTRODUCTION

Spontaneous Raman spectroscopy is usually not considered a viable quantitative technique, in part because the signal-to-noise ratio (S/N) of a Raman measurement is typically much poorer than that of mid-IR or near-IR methods. However, the poor S/N, as compared to near-

Received 12 September 1988; revision received 23 January 1989.
* Permanent address: Nuclear Research Centre, Beer-Sheva, Israel.
† Author to whom correspondence should be sent.

0003-7028/89/4306-1067$2.00/0